THE JOURNAL OF BIOLOGICAL CHEMISTRY VOL. 286, NO. 31, pp. 27573–27581, August 5, 2011

Superoxide Flashes

*EARLY MITOCHONDRIAL SIGNALS FOR OXIDATIVE STRESS-INDUCED APOPTOSIS**[S]

Received for publication, March 23, 2011, and in revised form, May 29, 2011 Published, JBC Papers in Press, June 9, 2011, DOI 10.1074/jbc.M111.241794

Qi Ma[‡§1], Huaqiang Fang[¶1], Wei Shang[¶], Lei Liu[‡§], Zhengshuang Xu[‖], Tao Ye[‖], Xianhua Wang[¶], Ming Zheng[¶2], Quan Chen[‡ ‡‡3], and Heping Cheng[¶]**

*From the [‡]Joint Laboratory of Apoptosis and Cancer Biology, State Key Laboratory of Biomembrane and Membrane Biotechnology, Institute of Zoology, Chinese Academy of Sciences, Beijing 100101, China, the [¶]Institute of Molecular Medicine and State Key Laboratory of Biomembrane and Membrane Biotechnology, Peking University, Beijing 100871, China, the [§]Graduate University of Chinese Academy of Sciences, Beijing 100049, China, the [‖]Laboratory of Chemical Genomics, Peking University Shenzhen Graduate School, Shenzhen 518055, China, the **Department of Applied Biology & Chemical Technology, The Hong Kong Polytechnic University, Hong Kong, China, and the [‡‡]Tianjin Key Laboratory of Protein Sciences, College of Life Sciences, Nankai University, Tianjin 300071, China*

Irreversible mitochondrial permeability transition and the resultant cytochrome *c* release signify the commitment of a cell to apoptotic death. However, the role of transient MPT (tMPT) because of flickering opening of the mitochondrial permeability transition pore remains elusive. Here we show that tMPT and the associated superoxide flashes (*i.e.* tMPT/superoxide flashes) constitute early mitochondrial signals during oxidative stress-induced apoptosis. Selenite (a ROS-dependent insult) but not staurosporine (a ROS-independent insult) stimulated an early and persistent increase in tMPT/superoxide flash activity prior to mitochondrial fragmentation and a global ROS rise, independently of Bax translocation and cytochrome *c* release. Selectively targeting tMPT/superoxide flash activity by manipulating cyclophilin D expression or scavenging mitochondrial ROS markedly impacted the progression of selenite-induced apoptosis while exerting little effect on the global ROS response. Furthermore, the tMPT/superoxide flash served as a convergence point for pro- and anti-apoptotic regulation mediated by cyclophilin D and Bcl-2 proteins. These results indicate that tMPT/superoxide flashes act as early mitochondrial signals mediating the apoptotic response during oxidative stress, and provide the first demonstration of highly efficacious local mitochondrial ROS signaling in deciding cell fate.

The mitochondrial permeability transition (MPT)[4] is crucial to many forms of programmed cell death or apoptosis (1). The progression of apoptosis can be divided into three distinct phases, initiation, commitment, and execution. Through integration of diverse intracellular signals, the MPT serves as a logic gate that, once switched-on, commits the cell to death. Specifically, the irreversible MPT causes massive release of cytochrome *c* and other apoptosis-inducing factors from the mitochondria into the cytoplasm (2–4), accompanied by an intense burst of reactive oxygen species (ROS) production (5). This critical transition occurs precipitously, completing within just a few minutes in a given cell (6). Subsequent execution of apoptosis invokes caspase pathways that are well conserved and relatively well-characterized in eukaryotes (7). By contrast, the process of cell fate decision prior to commitment appears to be highly heterogeneous, depending on the nature of the death-inducing insult. To date, it is unknown whether the MPT plays any role in the early initiation phase of any type of apoptosis. In addition, it remains controversial whether mitochondrial ROS is a causative factor in apoptosis or merely an inevitable consequence of damage manifesting in the form of a ROS burst at the juncture of commitment to cell death (8, 9).

The irreversible MPT reflects sustained opening of the mitochondrial permeability transition pore (mPTP), a voltage-dependent channel of still-elusive molecular identity. Three proteins, the voltage-dependent anion channel in the outer membrane, the adenine nucleotide translocator (ANT) in the inner membrane and cyclophilin D (CypD) on the matrix side, have been suggested as its main components or crucial regulators (10–13). In addition to the sustained mPTP opening that underlies irreversible MPT, it has also been shown that a transient MPT (tMPT) because of stochastic, flickering mPTP opening occurs incessantly in intact cells (14–16) and in *ex vivo* beating hearts, and gives rise to 10-s bursts of superoxide production in the matrix of the mitochondrion, dubbed "superoxide flashes" (14). Furthermore, the rate of superoxide flash production can be modulated by oxidative stress or metabolic status (14, 15). These recent findings raise the intriguing possibility that the mPTP, while in flickering gating mode, may regulate apoptosis at the initiation phase, and if so, may also serve as a point of convergence for the diverse signaling pathways that regulate cell survival and cell death.

By visualizing superoxide flashes simultaneously as optical measurements of tMPT activity and local mitochondrial ROS production events in HeLa cells, here we sought to determine

* This work was supported by grants from the National Science Foundation (90713006, 30971062, 30910103910, 30630021) the National Key Basic Research Program of China (2007CB512100, 2011CB809102, 2011CB910903, and 2010CB912204) and a special grant from State Key Laboratory of Biomembrane and Membrane Biotechnology.

[S] The on-line version of this article (available at http://www.jbc.org) contains supplemental Figs. S1–S5 and Movies S1–S3.

[1] Both authors contributed equally to this work.
[2] To whom correspondence may be addressed. E-mail: zhengm@pku.edu.cn.
[3] To whom correspondence may be addressed. E-mail: chenq@ioz.ac.cn.

[4] The abbreviations used are: MPT, mitochondrial permeability transition; tMPT, transient MPT; ROS, reactive oxygen species; DCF, dichlorodihydrofluorescein; mPTP, mitochondrial permeability transition pore; ANT, adenine nucleotide translocator; CypD, cyclophilin D.

the possible role of tMPT and the associated ROS signal in the process of mitochondrion-mediated intrinsic apoptosis. We found that superoxide flashes triggered by flickering mPTP openings constitute early and elemental signals for selenite- but not staurosporine-induced apoptosis, while paradoxically contributing little to the global ROS response. This finding not only establishes a heretofore unappreciated role of flickering mPTP in the regulation of cell fate, but also provides new insights into local mitochondrial ROS signaling.

EXPERIMENTAL PROCEDURES

Plasmids—Mt-cpYFP was generated as described previously (14), and inserted into pcDNA4-TO/B at the HindIII and EcoRV restriction sites. Human wild-type Bax, the C62/126S mutant, and cytochrome *c* constructs were generated as described previously (17), and inserted into pmCherry-C3 at the HindIII and EcoRI restriction sites.

Cell Culture and Transfection—Cells were all grown in Dulbecco's modified Eagle's medium supplemented with 10% fetal bovine serum and 1% penicillin and streptomycin at 37 °C under 5% CO_2. To establish stable cell lines, HeLa cells were transfected with mt-cpYFP or Bcl-2 plasmids, and positive clones were selected with 0.1 mg/ml zeocin or 2 μg/ml puromycin for 2 weeks. In a subset experiment, adenoviral mouse CypD was transiently transfected into HeLa cells for CypD overexpression.

Confocal Imaging of Living Cells—Cells were grown on 14-mm diameter glass-bottom microwell dishes. For tetramethyl rhodamine methyl ester (TMRM) and Rhod-2 loading and imaging, mt-cpYFP stable HeLa cells were incubated with 25 nM TMRM or 5 μM Rhod-2 for 30 min at 37 °C. For Bax transfer and cytochrome *c* release analysis, mt-cpYFP stable HeLa cells were transiently transfected with Bax-mCherry, C62/126S Bax-mCherry, or Cyt c-mCherry. Before experiments, cells were washed with Tyrode's solution (in mM: 137 NaCl, 20 HEPES, 10 D-glucose, 5.4 KCl, 1.2 $MgCl_2$, 1.2 NaH_2PO4, 1.8 $CaCl_2$, pH 7.4) and imaged at 37 °C under 5% CO_2, using a Zeiss LSM 510 confocal microscope. Real-time images were captured with a 40×, 1.3 NA oil-immersion objective at a sampling rate of 1.57 s/frame; dual excitation imaging of mt-cpYFP was achieved by alternating excitation at 405 and 488 nm, and collecting the emission at 500–550 nm; and excitation imaging of mCherry, TMRM or Rhod-2 was achieved at 543 nm, and the emission was collected at 565–615 nm. Digital image processing used IDL software and customer-devised programs.

Global ROS Measurement by Dichlorodihydrofluorescein (DCF) Assay—Cells were incubated with 10 μM CM-H_2DCFDA at 37 °C under 5% CO_2 for 15 min, then washed with PBS. The fluorescence was measured qualitatively by confocal microscopy under excitation at 488 nm, and the emission was collected at 500–550 nm. Cells treated with 0.1 μM H_2O_2 for 30 min were used as positive control.

Immunostaining—Cells cultured on coverslips were fixed with 3.7% formaldehyde at 37 °C for 15 min, and permeabilized with 0.2% Triton X-100 for 10 min. FITC-conjugated antibody was used to stain endogenous cytochrome *c*. For statistical analysis of cytochrome *c* release, cell images were captured by confocal microscopy with a 63×, 1.4 NA oil-immersion objective at a sampling rate of 15.7 s/frame.

RNA Interference Assay—Two sets of RNAi sequences for human cyclophilin D were used: #1 GGAGGACATCCAAGAAGAT and #2 GACGAGAACTTTACACTGA. Twenty nanomolar shRNA was transiently transfected into cells with Lipofectamine 2000, according to the manufacturer's instructions.

Immunoblotting—Cell lysates were subjected to SDS-PAGE and transferred onto nitrocellulose membranes. The membranes were then probed with the indicated antibodies, followed by appropriate HRP-conjugated secondary antibodies. Immunoreactive bands were visualized with enhanced chemiluminescence (ECL) reagents.

Flow Cytometric Assay for Apoptosis—Cells in 6-well plates were collected and washed with binding buffer (in mM: 10 HEPES, 140 NaCl, 5 $CaCl_2$, pH 7.4), then stained with Annexin V-FITC and propidium iodide (PI) for 20 min in the dark at room temperature. Flow cytometric analysis was performed to monitor the green fluorescence of the FITC (500–550 nm) and the red fluorescence of DNA-bound PI (565–615 nm). All data were analyzed with Cell Quest software (BD).

Reagents and Antibodies—Sodium selenite, staurosporine, cyclosporine A, anti-Flag monoclonal antibody, anti-β-actin monoclonal antibody, manganese (III) tetrakis (N-methyl-2-pyridyl) porphyrin (MnTMPyP), MnTBAP, and mitoTEMPO were from Sigma. 5- and -6-Chloromethyl-20,70-dichlorodihydrofluorescein diacetate (CM-H_2DCFDA) was from Molecular Probes (Eugene, OR). Lipofectamine 2000 was from Invitrogen (San Diego, CA). Anti-cyclophilin D monoclonal antibody was from Calbiochem (Darmstadt, Germany). Secondary antibodies were from Pharmingen (San Diego, CA). ECL reagents were from Pierce. All other chemicals were from Sigma unless otherwise specified.

Statistics—All statistical analyses are expressed as means ± S.E. Significant differences between values under different experimental conditions were determined by two-tailed Student's *t* test or ANOVA with repeated measures, and $p < 0.05$ was considered statistically significant.

RESULTS

Superoxide Flashes as Optical Measurements of tMPT in HeLa Cells—In HeLa cells stably expressing the superoxide biosensor mt-cpYFP (14), fluorescence seen at 405 nm or 488 nm excitation was localized to the mitochondria, overlapping that of TMRM (at 543 nm excitation), a mitochondrial membrane potential ($\Delta\Psi_m$) indicator (supplemental Fig. S1*a*). Time-lapse confocal imaging revealed random superoxide flash activity in both filiform mitochondria (Fig. 1*a*) and convoluted mitochondrial networks (Fig. 1*b*). Albeit differing in appearance, filiform and network superoxide flashes were indistinguishable in terms of amplitude and kinetics (supplemental Fig. S2): they rose to a peak amplitude of 0.35 ($\Delta F/F_0$) in ~5 s, and dissipated with a 50% decay time (T_{50}) of ~7 s. This result suggests that they are an elemental mitochondrial phenomenon irrespective of mitochondrial morphology. Indeed, the amplitude and kinetic properties of superoxide flashes in HeLa cells were similar to those

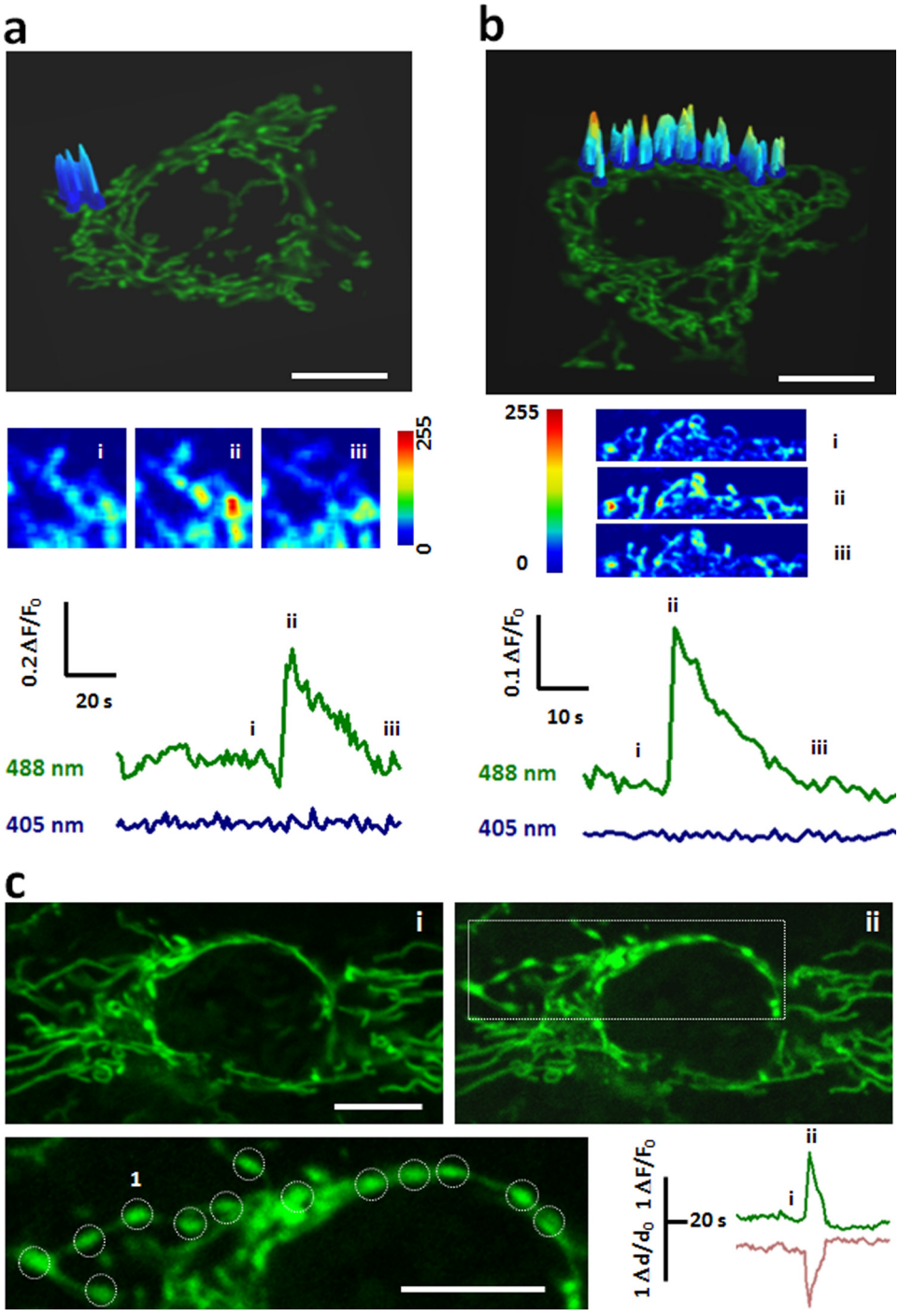

FIGURE 1. **Superoxide flashes in HeLa cells.** *a* and *b*, representative superoxide flashes in filiform (*a*) and network mitochondria (*b*). From *top to bottom*, confocal images of HeLa cells expressing mt-cpYFP, with overlay showing surface plots of the flashes at peak; enlarged and contrast enhanced views at designated time points (i, ii, iii); and time courses of mt-cpYFP fluorescence with dual excitation at 488 and 405 nm. Note that the fluorescence at 405 nm excitation is characteristically unchanged during a flash and is thus omitted from display elsewhere. *c*, local swelling of a network mitochondrion undergoing a superoxide flash. *Top panels* show views during quiescence (i) and at peak of the flash (ii). On the enlarged views of the boxed region, circles mark discrete loci of swelling. Paired traces show local changes of the mt-cpYFP signal (*upper trace*) and optically measured mitochondrial width (*lower trace*). Scale bars: 10 μm. See also supplemental Movies S1 and S2.

reported in muscle cells and cultured hippocampal neurons (14, 15).

Interestingly, we noted that conspicuous mitochondrial "contraction" often developed with the onset of the flash in a HeLa cell. In the network mitochondrion shown in Fig. 1*c*, spatiotemporal analysis demonstrated a synchronous flash and swelling at discrete loci separated by 3.2 ± 0.2 μm (Fig. 1*c*, and supplemental Movie S2). The swelling of flashing mitochondria was also observed at 405 nm excitation while the fluorescence intensity of cpYFP at this wavelength was largely unchanged (supplemental Fig. S1*b*), indicating that swelling-associated motion artifacts and possible indicator dilution had only limited effects on the cpYFP signal. This result supports the notion that tMPT causes mitochondrial swelling, masquerading as

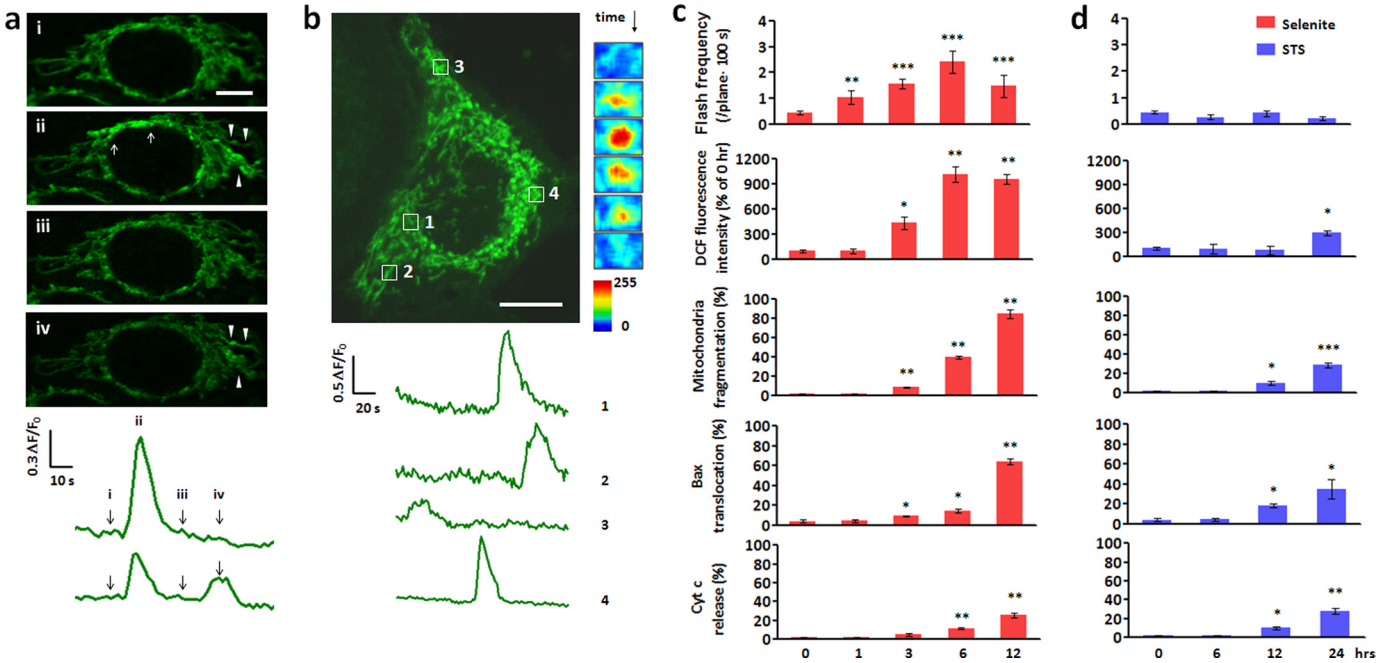

FIGURE 2. **Superoxide flashes in response to apoptotic insults.** *a*, early response to selenite. Time-lapse confocal images show two consecutive superoxide flashes (marked by *arrows* and *arrowheads*) in network mitochondria after 1 h selenite treatment (10 μM). Corresponding time course plots are shown at the *bottom*. *b*, persisting response 6 h after selenite treatment. Note the extensive mitochondrial fragmentation. Time courses of four superoxide flashes in punctiform mitochondria (marked by *boxes*) are plotted at the *bottom*, enlarged and contrast enhanced snapshots of a representative superoxide flash (1) are shown to the *right*. See also supplemental Movie S3. *c*, relationship between superoxide flash response and global ROS rise, mitochondrial fragmentation (the average mitochondrial length in a typical HeLa cell is 8 μm; mt-cpYFP HeLa cells with an average mitochondrial length of 2 μm were considered as fragmented, and the percentage of cells was calculated), Bax translocation or cytochrome *c* (*Cyt c*) release during selenite stimulation. *d*, as in *c*, during staurosporine stimulation (0.2 μM, STS). Scale bars: 10 μm. In *c* and *d*, global ROS was measured by the redox-sensitive dye CM-H_2DCFDA (DCF). Data are reported as mean ± S.E., $n = 34–84$ cells for frequency analysis; $n = 10^3$ cells from three experiments for global ROS detection. $n = 500$ cells from three experiments for mitochondrial fragmentation, Bax translocation or cytochrome *c* release. *, $p < 0.05$; **, $p < 0.01$; ***, $p < 0.001$ *versus* untreated cells.

mitochondrial contraction. Further evidence for the involvement of tMPT in superoxide flash production included concurrent loss of $\Delta\Psi_m$ (Fig. S1*a*) and irreversible loss of matrix-loaded rhod-2 ($M_r = 791$) (14, 18). Pharmacological inhibition of mPTP activity by cyclosporine A or bongkrekic acid, which acts on the putative CypD or ANT element of the mPTP complex (19), respectively, suppressed both filiform and network mitochondrial superoxide flashes (supplemental Fig. S1*c*). This result is consistent with our previous studies in cardiomyocytes and several other cell lines (14), but in contrast to adult skeletal muscle fibers where superoxide flash activity is cyclosporine A-independent (15). Together, the present and previous data suggest that CyPD is an important regulatory but nonessential component of the mPTP and different mechanisms underly superoxide flash activity depending on the cell type. Thus, in contrast to the irreversible MPT at the commitment to apoptotic cell death, single-mitochondrion superoxide flashes provide an optical readout of tMPTs that occur incessantly in intact HeLa cells, allowing for investigation of the roles of tMPT in apoptosis (see below).

Early and Persistent tMPT/Superoxide Flash Response to Oxidative Stress—Albeit local and brief, tMPT/superoxide flashes represent dramatic changes at the single mitochondrion level. Our central hypothesis was that such tMPT/superoxide flashes are early signals contributing to mitochondrial oxidative stress and apoptosis in the presence of apoptotic insults. In other words, flickering and sustained mPTP openings may play distinct yet complementary roles in the regulation of cell death. To test this hypothesis, we opted to challenge HeLa cells with selenite (10 μM) which, once diffused into the cell, increases O_2^- and other ROS and perturbs intracellular redox status, resulting in apoptotic cell death by ROS-dependent mechanisms (20, 21). As expected, selenite-induced cell death followed the canonical pattern of the apoptotic response, with the hallmarks of elevation of global ROS production (measured by fluorescence intensity of DCF), mitochondrial fragmentation, Bax translocation, and cytochrome *c* release, beginning at about 3 h after selenite treatment (Fig. 2*c*).

Interestingly, as early as 1 h after selenite treatment, we detected a robust 2.4-fold increase in tMPT/superoxide flash activity, prior to any appreciable changes in global ROS and mitochondrial morphology (Fig. 2, *a* and *c*). More network than filiform mitochondria were active in the presence of selenite, increasing the ratio of network:filiform flashes from 3:10 to 7:10 ($p < 0.05$, χ^2 test; supplemental Fig. S3*a*). However, the flash amplitude, rise time and decay kinetics remained unchanged (supplemental Fig. S2), indicating that selenite modulation of tMPT/superoxide flashes occurs mainly in a frequency-modulated (FM) fashion. Importantly, this tMPT/superoxide flash response was reversed upon selenite washout (supplemental Fig. S3*b*). These data indicate that an increase in tMPT/superoxide flash activity is an early cellular and mitochondrial response to selenite stimulation. Further, the temporal disparity between the superoxide flash response and the global ROS rise (Fig. 2*c*) suggests that superoxide flashes do not play any

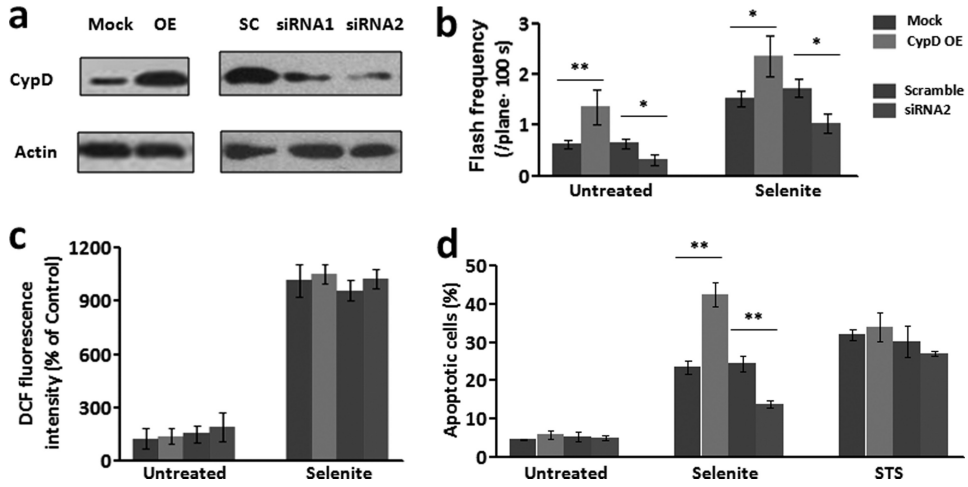

FIGURE 3. **CypD regulates superoxide flash activity and apoptosis.** *a*, Western blots for CypD protein levels after overexpression (*OE*) and knockdown of CypD (siRNA1 and siRNA2). *b*, superoxide flash frequency in CypD-manipulated cells, in the absence or presence of selenite (10 μM, 1–6 h). *c*, global ROS level was unaffected by CypD overexpression or knockdown, regardless of selenite treatment. *d*, overexpression of CypD exaggerated, and down-regulation of CypD ameliorated selenite (10 μM, 12 h) but not staurosporine (STS, 0.2 μM, 24 h)-induced apoptosis. Data are mean ± S.E., $n = 11–61$ cells for frequency analysis. $n = 10^4$ cells from three experiments for apoptosis assay. *, $p < 0.05$; **, $p < 0.01$ *versus* mock or scrambled controls. *Mock*, vector control; *OE*, overexpression of CypD; *SC*, scrambled CypD siRNA.

major role in directly contributing to global ROS homeostasis (see "Discussion").

Elevated tMPT/superoxide flash activity persisted during prolonged selenite stimulation, with peak activity attained 6 h after the onset of selenite treatment (Fig. 2*c*). As mitochondria were progressively fragmented, filiform and then punctiform tMPT/superoxide flashes became dominant (Fig. 2*b*): the proportions of network:filiform:punctiform events during early (0–6 h) and prolonged (6–12 h) treatment were 0.42:0.56:0.02 and 0.06:0.33:0.61, respectively, compared with 0.23:0.62:0.15 in untreated cells (supplemental Fig. S3a). As expected, tMPT/superoxide flashes vanished at 24 h, after irreversible MPT, complete loss of $\Delta\Psi_m$ and fully fledged cytochrome *c* release.

In contrast, staurosporine at 0.2 μM, which invokes ROS-independent programmed cell death (22) (32.0 ± 1.4% apoptotic cells at 24 h, Fig. 3*d*), failed to elicit any significant changes in tMPT/superoxide flash activity during the entire initiation phase of apoptosis (Fig. 2*d*). Nevertheless, cells subjected to staurosporine treatment underwent similar phases of mitochondrial fragmentation, Bax translocation, and cytochrome *c* release (Fig. 2*d*). Global ROS homeostasis was unperturbed until overt apoptosis (Fig. 2*d*), consistent with the late onset of irreversible mPTP opening and the associated global ROS burst (23). Altogether, our results show that the early response of tMPT/superoxide flashes is specifically linked to oxidative stress rather than general apoptotic insults.

Proapoptotic Effects of tMPT/Superoxide Flashes during Oxidative Stress—We next determined whether tMPT/superoxide flashes are causally linked to oxidative stress-induced apoptosis. To this end, we resorted to either siRNA interference or overexpression of CypD, a prominent regulator of the mPTP (22, 24). The two sets of siRNA (siRNA1 and siRNA2) displayed interference efficiency of 58 and 81%, respectively, at the protein level (Fig. 3*a*). Further experiments with siRNA2 revealed that down-regulation of CypD decreased spontaneous and selenite-induced tMPT/superoxide flash frequency by 51 and 41%, respectively (Fig. 3*b*). Remarkably, it retarded the progression of selenite-induced cell death, reducing apoptotic cells from 24.4 ± 2.1% to 13.8 ± 0.9% at 12 h treatment ($p < 0.05$, siRNA2 *versus* scrambled group) (Fig. 3*d*). Conversely, a 3-fold overexpression of CypD (24 h) caused a 2.6-fold increase in spontaneous tMPT/superoxide flashes, and a 1.5-fold elevation of early tMPT/superoxide flash responses to selenite treatment (0–6 h) (Fig. 3, *a* and *b*). Selenite-induced apoptotic cell death was exaggerated by 1.8-fold in CypD-overexpressing cells (42.4 ± 3.1% apoptotic cells at 12 h selenite stimulation) (Fig. 3*d*). Likewise, we found that CypD overexpression potentiated, and its knockdown diminished H_2O_2-induced cell apoptosis (supplemental Fig. S4*c*), and these effects occurred in parallel with changes in H_2O_2-stimulated superoxide flash activity (supplemental Fig. S4*a*), whereas the global ROS response was essentially unaffected by CypD manipulation (supplemental Fig. S4*b*). As compared with selenite causing similar level of cell death, the H_2O_2 treatment (120 μM) elicited relatively mild increase of superoxide flash activity (1.6-fold elevation at 6 h). This perhaps reflects the fact that, in addition to the intrinsic mitochondrial pathway, H_2O_2-induced cell death is also mediated by extrinsic pathways, including cell death receptors signaling (25), endoplasmic reticulum stress (26), and direct activation of Bax (17).

By contrast, cell death induced by staurosporine was essentially untouched by either CypD knockdown or overexpression (Fig. 3*d*), in general agreement with the fact that staurosporine induces cell death *via* a CsA-resistant and CypD-independent mechanism (22). It is noteworthy that in unchallenged cells, neither elevation of tMPT/superoxide flash activity by 2.6-fold with CypD overexpression nor its diminution by 51% with CypD knockdown caused any detectable change in cell death (Fig. 3*d*). This indicates that tMPT/superoxide flashes *per se* may not be sufficient to cause cell death; rather, they regulate apoptosis only in a context-sensitive manner. Taken together, our data indicate that CypD-dependent flickering mPTP opening serves as a proapoptotic signal in the presence of oxidative insults.

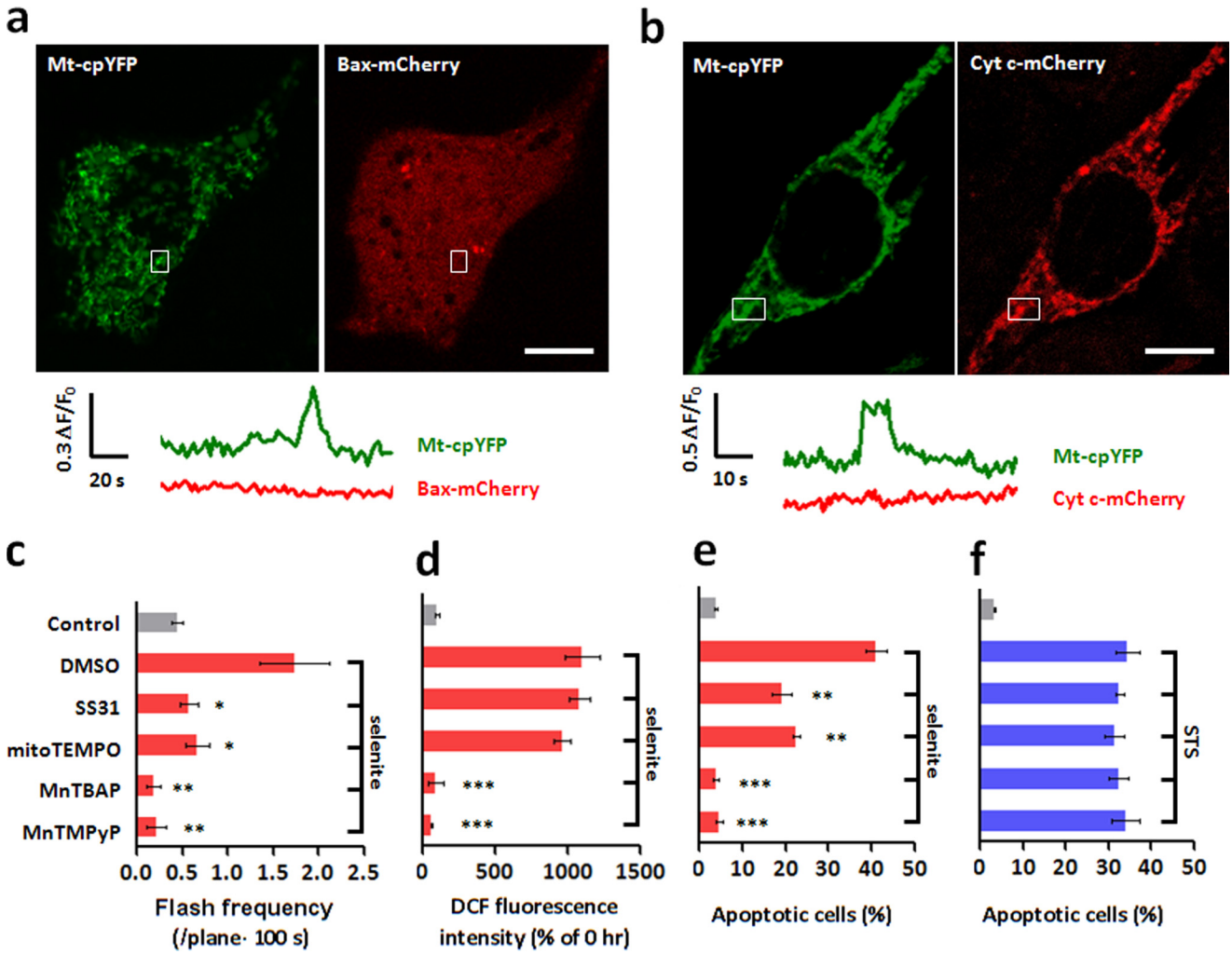

FIGURE 4. **Selenite-induced superoxide flashes are proapoptotic, acting independently of Bax translocation and cytochrome *c* release.** *a* and *b*, simultaneous measurement of superoxide flashes (mt-cpYFP) and the Bax-mCherry (*a*) or Cyt c-mCherry signal (*b*) 3 h after selenite treatment. Similar results were obtained in at least 30 cells. *c–f*, effects of targeting selectively on mitochondrial ROS (SS31, mitoTEMPO) or indiscriminately on global ROS (MnTBAP, MnTMPyP) on superoxide flashes (*c*), DCF fluorescence (*d*), selenite (10 μM, 24 h) (*e*), or staurosporine (0.2 μM, 24 h)-induced apoptosis (*f*). Scale bars: 10 μm. Data are reported as mean ± S.E., $n = 22–84$ cells for frequency analysis; $n = 10^3$ cells from three experiments for DCF and $n = 10^4$ cells for apoptosis assay. *, $p < 0.05$; **, $p < 0.01$; ***, $p < 0.001$ *versus* untreated cells.

Role of Local Mitochondrial ROS in Regulating Apoptosis—The question then arose of the specific mechanism whereby tMPT/superoxide flashes promote cell death. It has been well documented that irreversible mPTP opening instigates massive intracellular ROS production, triggers the translocation of the proapoptotic protein Bax from the cytosol to mitochondria, and causes the release of mitochondrial cell death factors including cytochrome *c* from the mitochondrial intermembrane space to the cytosol, thus committing the cell to death (27). We considered that the proapoptotic effect of tMPT/superoxide flashes might be mediated by similar mechanisms, only at the single mitochondrion level. We therefore determined whether flickering mPTP opening facilitates local Bax transfer or cytochrome *c* release. Bax-mCherry or Cyt c-mCherry was transiently expressed in the mt-cpYFP HeLa cell line. Simultaneous tracking of the Bax-mCherry signal and tMPT/superoxide flash activity revealed no detectable Bax translocation to the mitochondria undergoing superoxide flashes, regardless of selenite treatment (3–12 h) (Fig. 4*a*). Likewise, no detectable cytochrome *c* release accompanied superoxide flashes at the single mitochondrion level in the presence of selenite (Fig. 4*b*). The latter is in general agreement with the notion that flickering mPTP opening reflects a low-conductance state of the channel (28). These data exclude local Bax transfer or single-mitochondrion cytochrome *c* release as the mediator of the proapoptotic effect of tMPT/superoxide flashes.

We then investigated the possibility of local mitochondrial ROS, in the form of superoxide flashes, as an early signal for apoptosis. While our initial thought was that the sum of superoxide flashes could elevate the global ROS level and hence impact on apoptotic progression, our data showed that this was not the case. Bidirectional manipulation of tMPT/superoxide flash activity (by CypD knockdown or overexpression) neither alleviated nor aggravated the selenite- or H_2O_2-stimulated global ROS response (Fig. 3*c* and supplemental Fig. S4*b*), nor did it detectably perturb global ROS homeostasis in the absence of selenite or H_2O_2 stimulation (Fig. 3*c*). We then hypothesized that individual superoxide flashes can act locally at the single mitochondrion level, by analogy with the local calcium signal-

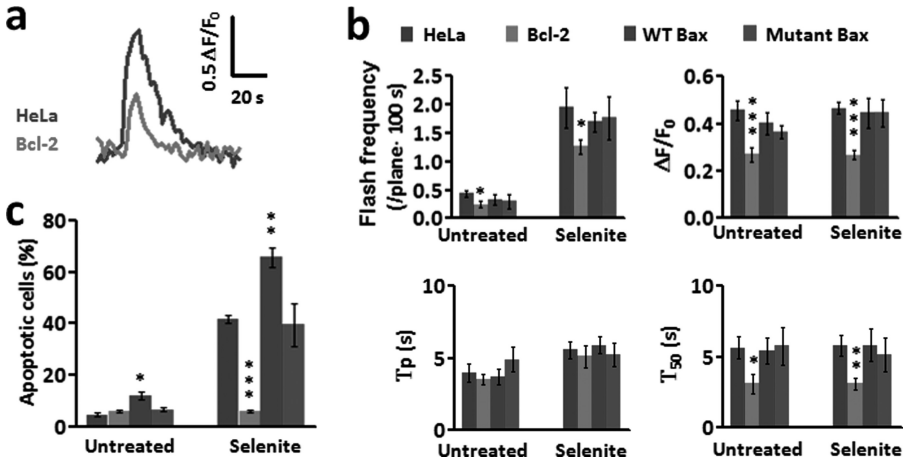

FIGURE 5. **Regulation of superoxide flash activity by Bcl-2 and Bax.** *a*, typical traces showing the inhibitory effect of Bcl-2 overexpression on superoxide flash amplitude and duration in the presence of selenite (10 μM, 6 h). *b*, effect of Bcl-2, Bax and mutant Bax (C62/126S) on superoxide flash properties in the absence or presence of selenite (10 μM, 6 h). $\Delta F/F_0$, amplitude; T_p, time to peak; T_{50}, 50% decay time. *c*, effect of Bcl-2, Bax, and C62/126S Bax on selenite (10 μM, 24 h)-induced apoptosis. Data are reported as mean ± S.E., $n = 20-60$ cells for frequency analysis; $n = 10^4$ cells for apoptosis assay. *, $p < 0.05$; **, $p < 0.01$; ***, $p < 0.001$, Bcl-2, Bax, and C62/126S Bax cells were compared with wild-type HeLa cells.

ing mechanism whereby miniscule amounts of calcium ions in high-concentration microdomains may have prominent cellular effects (29–32). To dissect the contribution of local mitochondrial ROS to apoptosis, we used two categories of ROS scavengers, those targeting specifically to the mitochondria (*i.e.* mitoTEMPO (33) and tetrapeptide D-Arg-Dmt-Lys-Phe-NH_2, the latter also known as SS31 (34)), and those indiscriminate with regard to local and global ROS (*i.e.* MnTMPyP and MnTBAP) (35). In the presence of selenite, MnTMPyP and MnTBAP completely abolished the global ROS rise as well as the increase of tMPT/superoxide flash activity (Fig. 4, *c* and *d*) and fully protected cells from selenite-induced apoptosis (Fig. 4*e*), consistent with previous reports (36). In contrast, SS31 and mitoTEMPO suppressed superoxide flash activity by 67 and 62% without perturbing the global ROS response (Fig. 4, *c* and *d*), and ameliorated apoptosis by 53 and 45%, respectively (Fig. 4*e*). Staurosporine-induced cell death, however, was insensitive to ROS scavengers in either category (Fig. 4*f*). These results indicate that local mitochondrial ROS signals, in the form of superoxide flashes, are crucial for selenite- but not staurosporine-induced apoptosis.

Bcl-2 Inhibition of tMPT/Superoxide Flashes: New Insights into Its Antiapoptotic Mechanism—Bcl-2 is a prototypic antiapoptotic protein, yet its mechanism of cell protection is not fully understood. To test if Bcl-2 regulates apoptosis by modulating flickering mPTP and tMPT/superoxide flash activity at the initiation phase, we established a HeLa cell line stably expressing Flag-tagged human Bcl-2 (Bcl-2-flag) (supplemental Fig. S5*a*) in conjunction with transient expression of mt-cpYFP. Our results showed that Bcl-2 profoundly inhibited both basal and selenite-induced flicking mPTP opening activity (Fig. 5*a*). Specifically, Bcl-2 overexpression, in cells with or without selenite, suppressed the occurrence of tMPT/superoxide flashes by 44 and 35%, respectively, as compared with wild-type cells (Fig. 5*b*). The remaining tMPT/superoxide flash events were much tinier and briefer, with $\Delta F/F_0$ diminished by about 60% and T_{50} abbreviated by about 50% (Fig. 5*b*), indicative of both FM and amplitude-modulated (AM) effects. The Bcl-2 inhibition of tMPT/superoxide flashes was accompanied by complete protection against selenite-induced cell death (Fig. 5*c*). This result demonstrates that Bcl-2 acts constantly through the entire initiation phase by suppressing the tMPT/superoxide flash response to selenite stimulation, contributing at least in part to its antiapoptotic effect.

Bax, a proapoptotic protein of the Bcl-2 family, is thought to act late during the apoptotic process by forming a supramolecular opening at the outer mitochondrial membrane, bypassing the mPTP (37, 38). Overexpression of Bax by 2.5-fold or a similar level of expression of its C62/126S mutant (17) (as a control) (supplemental Fig. S5*b*) altered neither basal nor selenite-induced tMPT/superoxide flash activity (Fig. 5*b*). This finding is consistent with the lack of Bax involvement in the early phase of cell death and substantiates its action by an mPTP-independent mechanism.

DISCUSSION

In the present study, we have shown, for the first time, that flickering mPTP opening and the associated superoxide flashes are essential signals at the early stage of certain types of apoptosis, in contrast to the well-established role of sustained mPTP opening in the commitment to apoptotic cell death. Several lines of evidence support the proapoptotic role of local mitochondrial ROS in the presence of oxidative stress. First, tMPT/superoxide flashes were among the first responders to the apoptotic insult. They increased early in response to selenite stimulation, prior to global ROS elevation, mitochondrial fragmentation and other hallmarks of cellular commitment to death. Together with the reversibility of the tMPT/superoxide flash response to 1-h selenite treatment, this result suggests that the tMPT/superoxide flash response is among the most proximal signaling events in the progression of apoptotic cell death. Second, tMPT/superoxide flashes are causally linked to the apoptotic effects induced by oxidative insult. Increasing or suppressing tMPT/superoxide flashes bidirectionally regulated the progression of apoptosis. Quantitatively, a 67, 62, or 41% inhibition of the superoxide flash response by SS31, mito-

TEMPO or CypD knockdown provided nearly proportional 53, 45, or 43% cell protection, respectively; whereas a 1.5-fold increase of flashes by CypD overexpression potentiated the selenite-induced cell death by 1.8-fold. Thus, the mPTP plays distinct yet complementary roles by causing transient or irreversible MPT at different phases of apoptotic cell death. Mechanistically, the proapoptotic effect of tMPT/superoxide flashes occurs independently of Bax transfer or cytochrome *c* release; rather, it critically depends on local mitochondrial ROS signals, the superoxide flashes.

Linking tMPT/superoxide flashes to the early signal of apoptosis has allowed for new insights into pro- and anti-apoptotic mechanisms. For instance, the present results indicate that down-regulation of CypD protects the cell and, conversely, overexpression of CypD exaggerates the apoptosis induced by oxidative stress. While this proapoptotic effect of CypD might be expected from CypD regulation of irreversible MPT (22, 24), our data have pinpointed that CypD manipulation impacts early at the initiation phase of apoptosis by promoting the tMPT/superoxide flash response to selenite. Notably, the CypD effect occurs in an FM mode, altering the propensity for flash occurrence without affecting the unitary properties of individual events. Likewise, the antiapoptotic protein Bcl-2 exerts an early and profound modulatory effect on flickering mPTP opening in response to oxidative stress. However, the Bcl-2 effect occurs in both FM and AM modes: overexpression of Bcl-2 not only diminishes the rate of occurrence of tMPT/superoxide flashes, but also decreases the flash amplitude and abbreviates their duration, as if Bcl-2 acts as a direct regulator of the mPTP complex (39–41). This component of the Bcl-2 protective effect should occur throughout the entire initiation phase, complementary to Bcl-2 binding of Bax and Bak to prevent the formation of a mitochondrial outer membrane pore at the phase of commitment (27). It has been controversial whether the mPTP is involved in Bax-mediated proapoptotic mechanisms (38–40, 42). Our data show that the proapoptotic effect of Bax is independent of tMPT/superoxide flashes, suggesting that Bax bypasses the mPTP, at least in the early phase of apoptotic signal transduction. Thus, real-time visualization of tMPT/superoxide flashes offers a new means for the elucidation of specific mechanisms for diverse regulators of cell death.

We have also appraised the relationship between mitochondrial ROS (in the form of superoxide flashes) and global ROS (as measured by DCF fluorescence) at the early stage of oxidative stress-induced apoptosis, and revealed a number of surprising findings. First, intermittent local superoxide flashes make only a miniscule contribution to the time-averaged global ROS level or global ROS rise during selenite stimulation. This is somewhat unexpected but can be accounted for by the spatial confinement, temporal brevity, and low frequency of superoxide flashes. In addition, it may also stem from the powerful ROS scavenging that is collectively determined by superoxide dismutases, catalase, peroxidases, and glutathione in the milieu of an intact cell (32, 43). Secondly, that such a local mitochondrial ROS signal is an essential component of the early signaling cascade of apoptosis (see above) attests to the efficiency of high ROS microdomains, analogous to that of high calcium microdomains (29–32). In other words, superoxide flashes represent quintessential *local* ROS signals, akin to elemental calcium signals (*e.g.* sparks, sparklets, puffs, and flickers) (44, 45). In the presence of an apoptotic insult, elemental mitochondrial signals accumulate over the many hours of the initiation phase, leading to the commitment to apoptosis. Thirdly, it appears that superoxide flashes are necessary, but not sufficient, signals for oxidative stress-induced apoptosis. This finding is in general agreement with the emerging dichotomy of ROS signaling in physiology and pathophysiology. Alternatively, there might be a threshold level of intensity for the manifestation of the proapoptotic effect of the superoxide flashes.

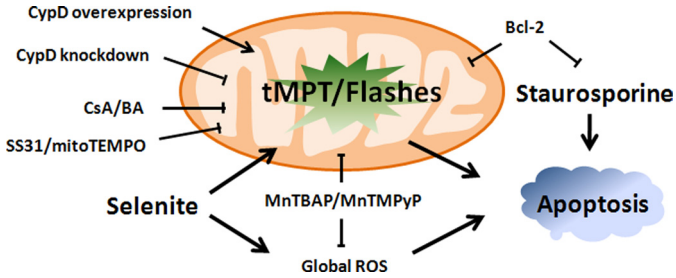

FIGURE 6. **Schematic diagram of superoxide flash regulation of apoptosis.** Local mitochondrial ROS, in the form of superoxide flashes, is essential for ROS-dependent (triggered by selenite) but not ROS-independent apoptosis (triggered by staurosporine), and serves as a point of convergence for many antiapoptotic (*e.g.* SS31, CsA, Bcl-2) and proapoptotic (*e.g.* CypD, but not Bax) mechanisms.

In contrast to the present finding that tMTP/superoxide flashes serve as essential signals for initiation of selenite-induced apoptosis, previous studies on cardiac preconditioning revealed protective effect of tMPT against ischemia/reperfusion injury (46, 47). The apparent discrepancy further underscores opposing role of tMPT and ROS in cell fate regulation, depending on the magnitude and duration of increased tMPT and ROS activity as well as the condition of the cell. Indeed, it has been shown that sustained increase of ROS leads to death of cardiomyocytes, while repetitive brief episodes of ROS treatment confer cardio protective effect against ischemia/reperfusion injury (46, 48, 49).

In summary, we have demonstrated that superoxide flashes due to flickering mPTP openings act as early and elemental mitochondrial ROS signals underlying oxidative stress-induced apoptosis in HeLa cells. Different pro- and anti-apoptotic mechanisms converge on the tMPT/superoxide flash activity while displaying distinctive modes of action (Fig. 6). The disparity between the profound proapoptotic effect of superoxide flashes and their tiny contribution to the global ROS response underscores the high signaling efficiency of local mitochondrial ROS signals in determining cell fate. Selectively targeting the tMPT/superoxide flash activity, with minimal perturbation of global ROS homeostasis, holds promise for the development of new treatments for a wide variety of oxidative stress-related diseases.

Acknowledgment—We thank Iain Bruce for editing the manuscript.

REFERENCES

1. Kroemer, G., Galluzzi, L., and Brenner, C. (2007) *Physiol. Rev.* **87,** 99–163
2. Li, L. Y., Luo, X., and Wang, X. (2001) *Nature* **412,** 95–99

3. Candé, C., Vahsen, N., Kouranti, I., Schmitt, E., Daugas, E., Spahr, C., Luban, J., Kroemer, R. T., Giordanetto, F., Garrido, C., Penninger, J. M., and Kroemer, G. (2004) *Oncogene* **23,** 1514–1521
4. Yang, J., Liu, X., Bhalla, K., Kim, C. N., Ibrado, A. M., Cai, J., Peng, T. I., Jones, D. P., and Wang, X. (1997) *Science* **275,** 1129–1132
5. Zorov, D. B., Filburn, C. R., Klotz, L. O., Zweier, J. L., and Sollott, S. J. (2000) *J. Exp. Med.* **192,** 1001–1014
6. Goldstein, J. C., Waterhouse, N. J., Juin, P., Evan, G. I., and Green, D. R. (2000) *Nat. Cell Biol.* **2,** 156–162
7. Green, D. R., and Reed, J. C. (1998) *Science* **281,** 1309–1312
8. Lin, M. T., and Beal, M. F. (2006) *Nature* **443,** 787–795
9. Stowe, D. F., and Camara, A. K. (2009) *Antioxid. Redox Signal.* **11,** 1373–1414
10. Desagher, S., and Martinou, J. C. (2000) *Trends Cell Biol.* **10,** 369–377
11. Crompton, M., Barksby, E., Johnson, N., and Capano, M. (2002) *Biochimie* **84,** 143–152
12. Shimizu, S., Narita, M., and Tsujimoto, Y. (1999) *Nature* **399,** 483–487
13. Marzo, I., Brenner, C., Zamzami, N., Jürgensmeier, J. M., Susin, S. A., Vieira, H. L., Prévost, M. C., Xie, Z., Matsuyama, S., Reed, J. C., and Kroemer, G. (1998) *Science* **281,** 2027–2031
14. Wang, W., Fang, H., Groom, L., Cheng, A., Zhang, W., Liu, J., Wang, X., Li, K., Han, P., Zheng, M., Yin, J., Mattson, M. P., Kao, J. P., Lakatta, E. G., Sheu, S. S., Ouyang, K., Chen, J., Dirksen, R. T., and Cheng, H. (2008) *Cell* **134,** 279–290
15. Pouvreau, S. (2010) *PLoS One* **5,** 13035–13037
16. Petronilli, V., Miotto, G., Canton, M., Brini, M., Colonna, R., Bernardi, P., and Di Lisa, F. (1999) *Biophys. J.* **76,** 725–734
17. Nie, C., Tian, C., Zhao, L., Petit, P. X., Mehrpour, M., and Chen, Q. (2008) *J. Biol. Chem.* **283,** 15359–15369
18. Hajnóczky, G., Robb-Gaspers, L. D., Seitz, M. B., and Thomas, A. P. (1995) *Cell* **82,** 415–424
19. Bernardi, P. (1996) *Biochim. Biophys. Acta* **1275,** 5–9
20. Nilsonne, G., Sun, X., Nyström, C., Rundlöf, A. K., Potamitou Fernandes, A., Björnstedt, M., and Dobra, K. (2006) *Free Radic. Biol. Med.* **41,** 874–885
21. Zhao, R., Xiang, N., Domann, F. E., and Zhong, W. (2006) *Cancer Res.* **66,** 2296–2304
22. Baines, C. P., Kaiser, R. A., Purcell, N. H., Blair, N. S., Osinska, H., Hambleton, M. A., Brunskill, E. W., Sayen, M. R., Gottlieb, R. A., Dorn, G. W., Robbins, J., and Molkentin, J. D. (2005) *Nature* **434,** 658–662
23. Chen, Q., Chai, Y. C., Mazumder, S., Jiang, C., Macklis, R. M., Chisolm, G. M., and Almasan, A. (2003) *Cell Death Differ.* **10,** 323–334
24. Schinzel, A. C., Takeuchi, O., Huang, Z., Fisher, J. K., Zhou, Z., Rubens, J., Hetz, C., Danial, N. N., Moskowitz, M. A., and Korsmeyer, S. J. (2005) *Proc. Natl. Acad. Sci. U.S.A.* **102,** 12005–12010
25. Pallepati, P., and Averill-Bates, D. A. (2011) *Free Radic. Biol. Med.* **50,** 667–679
26. Wei, H., Li, Z., Hu, S., Chen, X., and Cong, X. (2010) *J. Cell. Biochem.* **111,** 967–978
27. Wang, X. (2001) *Genes Dev.* **15,** 2922–2933
28. Zoratti, M., and Szabò, I. (1995) *Biochim. Biophys. Acta* **1241,** 139–176
29. Cheng, H., Lederer, W. J., and Cannell, M. B. (1993) *Science* **262,** 740–744
30. Lipp, P., and Niggli, E. (1998) *J. Physiol.* **508,** 801–809
31. Wang, S. Q., Song, L. S., Lakatta, E. G., and Cheng, H. (2001) *Nature* **410,** 592–596
32. Dröge, W. (2002) *Physiol. Rev.* **82,** 47–95
33. Dikalova, A. E., Bikineyeva, A. T., Budzyn, K., Nazarewicz, R. R., McCann, L., Lewis, W., Harrison, D. G., and Dikalov, S. I. (2010) *Circ. Res.* **107,** 106–116
34. Zhao, K., Zhao, G. M., Wu, D., Soong, Y., Birk, A. V., Schiller, P. W., and Szeto, H. H. (2004) *J. Biol. Chem.* **279,** 34682–34690
35. Hoehn, K. L., Salmon, A. B., Hohnen-Behrens, C., Turner, N., Hoy, A. J., Maghzal, G. J., Stocker, R., Van Remmen, H., Kraegen, E. W., Cooney, G. J., Richardson, A. R., and James, D. E. (2009) *Proc. Natl. Acad. Sci. U.S.A.* **106,** 17787–17792
36. Huang, F., Nie, C., Yang, Y., Yue, W., Ren, Y., Shang, Y., Wang, X., Jin, H., Xu, C., and Chen, Q. (2009) *Free Radic. Biol. Med.* **46,** 1186–1196
37. Kuwana, T., Mackey, M. R., Perkins, G., Ellisman, M. H., Latterich, M., Schneiter, R., Green, D. R., and Newmeyer, D. D. (2002) *Cell* **111,** 331–342
38. Eskes, R., Antonsson, B., Osen-Sand, A., Montessuit, S., Richter, C., Sadoul, R., Mazzei, G., Nichols, A., and Martinou, J. C. (1998) *J. Cell Biol.* **143,** 217–224
39. Brenner, C., Cadiou, H., Vieira, H. L., Zamzami, N., Marzo, I., Xie, Z., Leber, B., Andrews, D., Duclohier, H., Reed, J. C., and Kroemer, G. (2000) *Oncogene* **19,** 329–336
40. Shimizu, S., Eguchi, Y., Kamiike, W., Funahashi, Y., Mignon, A., Lacronique, V., Matsuda, H., and Tsujimoto, Y. (1998) *Proc. Natl. Acad. Sci. U.S.A.* **95,** 1455–1459
41. Shimizu, S., Konishi, A., Kodama, T., and Tsujimoto, Y. (2000) *Proc. Natl. Acad. Sci. U.S.A.* **97,** 3100–3105
42. Wei, M. C., Zong, W. X., Cheng, E. H., Lindsten, T., Panoutsakopoulou, V., Ross, A. J., Roth, K. A., MacGregor, G. R., Thompson, C. B., and Korsmeyer, S. J. (2001) *Science* **292,** 727–730
43. Circu, M. L., and Aw, T. Y. (2010) *Free Radic. Biol. Med.* **48,** 749–762
44. Wei, C., Wang, X., Chen, M., Ouyang, K., Song, L. S., and Cheng, H. (2009) *Nature* **457,** 901–905
45. Cheng, H., and Lederer, W. J. (2008) *Physiol. Rev.* **88,** 1491–1545
46. Saotome, M., Katoh, H., Yaguchi, Y., Tanaka, T., Urushida, T., Satoh, H., and Hayashi, H. (2009) *Am. J. Physiol. Heart Circ. Physiol.* **296,** H1125–H1132
47. Hausenloy, D., Wynne, A., Duchen, M., and Yellon, D. (2004) *Circulation* **109,** 1714–1717
48. Yaguchi, Y., Satoh, H., Wakahara, N., Katoh, H., Uehara, A., Terada, H., Fujise, Y., and Hayashi, H. (2003) *Circ. J.* **67,** 253–258
49. Tritto, I., D'Andrea, D., Eramo, N., Scognamiglio, A., De Simone, C., Violante, A., Esposito, A., Chiariello, M., and Ambrosio, G. (1997) *Circ. Res.* **80,** 743–748